Supporting Information

Photoactivation Properties of Self-n-Doped Perylene Diimides: Concentration-Dependent Radical Anion and Dianion Formation

Daniel Powell[1], Zayn Rhodes[1], Xinwen Zhang[2], Edwin J. Miller[1], McKenzie Jonely[1], Kameron R. Hansen[1], Chideraa I. Nwachukwu[1], Andrew G. Roberts[1], He Wang[2], Rodrigo Noriega[1], Shelley D. Minteer[1], Luisa Whittaker-Brooks[1,*]

1. *Department of Chemistry, University of Utah, Salt Lake City, Utah, 84112, United States*
2. *Department of Physics, University of Miami, Coral Gables, Florida, 33146, United States*

Table of Contents

Section 1. Synthesis and photoactivation

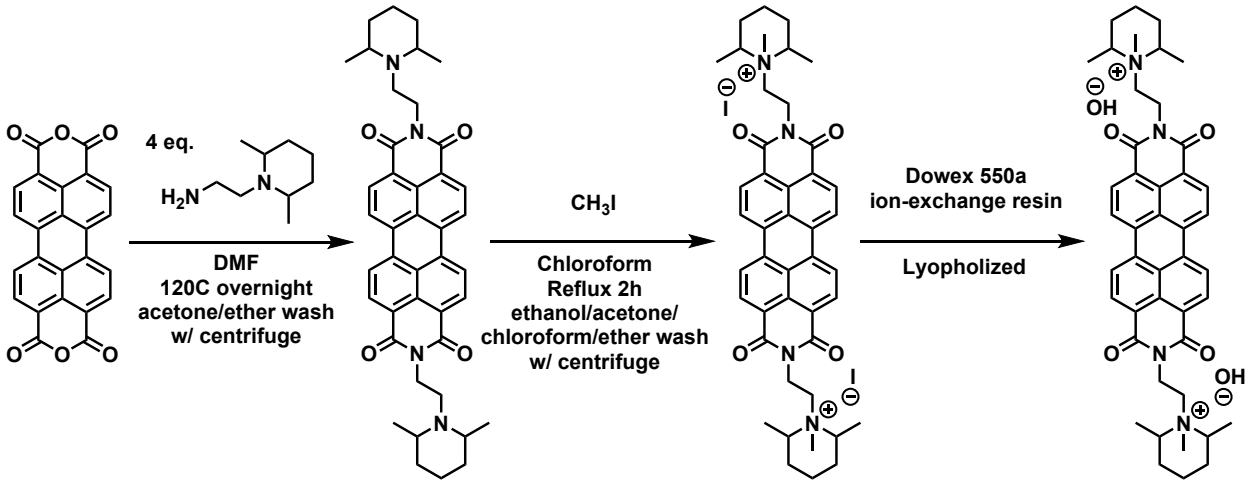

Scheme S1. Generalizable three step reaction scheme for the synthesis of self-n-doped PDIs. Here, the synthesis of D2I and D2OH are shown.

All compounds used in this study were synthesized by adapting methods from previously published procedures.[1,2] A generalized reaction scheme is presented below. This same scheme was used for all materials in this work. Briefly, 4 equivalents of the desired self-dopant, such as 2-(2,6-dimethylpiperidin-1-yl)ethan-1-amine (2 mmol) was added to 1 equivalent of perylene-3,4,9,10-tetracarboxylic dianhydride (0.5 mmol) and suspended in dimethyl formamide (DMF) (20 mM) in a round-bottom flask equipped with a condenser and stirred overnight at 120 °C. Upon cooling to room-temperature, 50 mL of acetone was added to the mixture and allowed to stand for 10 minutes. The slurry was then transferred to a centrifuge tube and centrifuged at 6000 rpm for 2 minutes and the supernatant was decanted. All solids were subsequently re-suspended and centrifuged 3 times with both acetone and diethyl ether (50 mL each wash), and dried under vacuum to yield a red solid. The product (0.5 mmol) was then dissolved in chloroform (20 mM) in a round-bottom flask and 2 equivalents of iodomethane (1 mmol) were added. The reaction mixture was refluxed for 2 hours and then cooled to room-temperature. The product (D2I) was then washed several times with

chloroform, ethanol, acetone, and ether in a centrifuge tube and dried under vacuum to yield a reddish black solid. To obtain D2OH, a dilute solution (~90 μM) of D2I was prepared in 18 MΩ-cm ultrapure water. A column was loaded with an excess of Dowex Monosphere 550a ion exchange resin, and the D2I solution was allowed to slowly pass through the column using only gravity three times, and the water was then removed with an SP VirTis benchtop lyopholizer to yield a fluffy dark purple solid. All final products were immediately transferred to an N_2 filled glovebox after drying.

NMR spectra were collected at room temperature on either a Varian 400 MHz Unity INOVA spectrometer or 500 MHz VXR-class spectrometer. Mass spectrometry data were collected using a Waters Xevo G2-S quadrupole time-of-flight mass spectrometer. Mass spectra were collected in positive ion mode, with the following parameters: 3 kV capillary voltage; 25 V sampling cone voltage; 120 °C source temperature; 350 °C desolvation temperature; nitrogen desolvation at 800 L/hr. The acquired mass spectra were processed using Masslynx 4.1 software. The authors note that the samples with hydroxide counterions are strongly paramagnetic, whereas the free amines and samples with iodide counterions are largely neutral. Thus, samples with hydroxide counterions may be reported as relatively broad regions. Mass spectra were obtained at the Mass Spectrometry Facility at the University of Utah. NMR spectra are reported in parts per million (ppm) relative to the residual protons of $CHCl_3$ (7.26 ppm) in $CDCl_3$, DMSO (2.50 ppm) in DMSO-d_6, or H_2O (4.79 ppm) in D_2O.

Bis[2-(dimethylamino)ethyl]perylene diimide, A2.

^{1}H NMR (500 MHz, $CDCl_3$) δ 8.69 (d, J = 7.9 Hz, 4H), 8.62 (d, J = 8.0 Hz, 4H), 4.37 (t, J = 7.0 Hz, 4H), 2.70 (t, J = 7.0 Hz, 4H), 2.37 (s, 12H). **^{13}C NMR** (126 MHz, $CDCl_3$) δ 163.50, 134.75,

131.55, 129.40, 127.20, 123.34, 123.16, 57.04, 45.82, 38.42. **MS** m/z calculated, 532.21; found, 533.3.

Bis[2-(piperidyn-1-yl)ethyl]perylene diimide, B2.

^{1}H NMR (500 MHz, $CDCl_3$) δ 8.64 (d, J = 7.9 Hz, 4H), 8.55 (d, J = 8.1 Hz, 4H), 4.40–4.36 (m, 4H), 2.73–2.67 (m, 4H), 2.58 (s, 8H), 1.63–1.58 (m, 8H), 1.48–1.43 (m, 4H). **^{13}C NMR** (126 MHz, $CDCl_3$) δ 163.20, 134.34, 131.18, 129.20, 126.17, 123.21, 122.92, 56.33, 54.80, 37.82, 26.07, 24.38. **MS** m/z $[M]^+$ calculated, 612.27; found, 613.4.

Bis[2-(diisopropylamino)ethyl]perylene diimide, C2.

^{1}H NMR (500 MHz, $CDCl_3$) δ 8.71 (d, J = 8.0 Hz, 4H), 8.66 (d, J = 8.1 Hz, 4H), 4.21 (t, J = 7.8 Hz, 4H), 3.12–3.06 (m, 4H), 2.75 (t, J = 7.8 Hz, 4H), 1.07 (d, J = 6.5 Hz, 24H). **^{13}C NMR** (126 MHz, $CDCl_3$) δ 167.81, 135.24, 132.45, 130.92, 128.83, 125.03, 123.20, 68.17, 38.72, 30.36, 28.94. **MS** m/z $[M]^+$ calculated, 644.34; found, 645.3.

Bis[2-(2,6-dimethylpiperidin-1-yl)ethyl]perylene diimide, D2.

^{1}H NMR (500 MHz, $CDCl_3$) δ 8.73 (d, J = 7.9 Hz, 4H), 8.68 (d, J = 8.2 Hz, 4H), 4.36 (s, 4H), 3.08 (s, 4H), 2.70 (s, 4H), 1.45 (s, 12H), 1.25 (d, J = 20.6 Hz, 8H), 0.09 (s, 4H). **^{13}C NMR** (126 MHz, $CDCl_3$) δ 167.80, 163.47, 132.45, 130.92, 129.43, 128.82, 123.31, 38.72, 30.36, 28.94, 23.02, 14.10, 10.99. **MS** m/z $[M]^+$ calculated, 668.34; found, 669.3434.

Bis[2-(trimethylammonium)ethyl]perylene diimide diiodide, A2I.

^{1}H NMR (500 MHz, DMSO) δ 8.79 (d, J = 8.0 Hz, 4H), 8.50 (d, J = 7.9 Hz, 4H), 4.50 (t, J = 7.3 Hz, 4H), 3.67 (t, J = 7.3 Hz, 4H), 3.24 (s, 18H). **^{13}C NMR** (126 MHz, DMF) δ 163.35, 134.99, 131.45, 129.31, 126.36, 124.52, 123.19, 62.77, 56.76, 52.93. **MS** m/z $[M\text{-}2I]^{2+}$ calculated, 281.13; found, 281.1293.

Bis[2-(1-methylpiperidyn-1-yl)ethyl]perylene diimide diiodide, B2I.

^{1}H NMR (500 MHz, DMSO) δ 8.87 (d, *J* = 8.3 Hz, 4H), 8.55 (d, *J* = 7.9 Hz, 4H), 4.48 (t, *J* = 7.6 Hz, 4H), 3.66 (t, *J* = 7.7 Hz, 4H), 3.60 – 3.44 (m, 8H), 3.23 (s, 6H), 1.86 (m, 8H), 1.58 (m, 4H). **^{13}C NMR** (126 MHz, DMF) δ 163.22, 134.77, 131.31, 128.58, 126.13, 124.45, 123.00, 61.24, 58.33, 51.98, 48.39, 20.91, 19.86. **MS** m/z $[M-2I]^{2+}$ calculated, 321.17; found, 321.1604.

Bis[2-(diisopropyl(methyl))ethyl]perylene diimide diiodide, C2I.

^{1}H NMR (500 MHz, D_2O) δ 8.40 (s, 4H), 7.87 (s, 4H), 4.17 (s, 4H), 3.21 (s, 6H), 2.88 (d, *J* = 78.1 Hz, 4H), 2.17 (s, 4H), 1.66 (s, 24H). **^{13}C NMR** (126 MHz, DMF) δ 162.86, 133.94, 130.98, 128.33, 125.13, 124.24, 122.18, 64.31, 52.74, 43.76, 17.33, 16.82. **MS** m/z $[M-2I]^{2+}$ calculated, 337.19; found, 337.1916.

Bis[2-(1,2,6-trimethylpiperidin-1-yl)ethyl]perylene diimide diiodide, D2I.

^{1}H NMR (500 MHz, $CDCl_3$) δ 8.69 (d, *J* = 7.8 Hz, 4H), 8.63 (d, *J* = 8.2 Hz, 4H), 4.78 – 4.64 (m, 6H), 1.60 (dp, *J* = 19.7, 7.0 Hz, 8H), 1.36 – 1.13 (m, 12H), 0.84 (ddt, *J* = 20.8, 17.3, 6.3 Hz, 16H). **^{13}C NMR** (126 MHz, DMF) δ 163.19, 134.19, 131.23, 128.60, 125.35, 124.39, 122.37, 79.45, 66.16, 54.49, 37.06, 28.08, 22.13, 15.11. **MS** m/z $[M-2I]^{2+}$ calculated, 349.19; found, 349.1912.

Bis[2-(trimethylammonium)ethyl]perylene diimide dihydroxide, A2OH.

^{1}H NMR (500 MHz, D_2O) δ 7.96 – 7.76 (m, 4H), 7.60 – 7.36 (m, 4H), 4.70 (s, 4H), 3.22 (s, 18H), 2.17 (d, *J* = 0.9 Hz, 4H). **^{13}C NMR** (126 MHz, D_2O) δ 215.42, 161.19, 138.57, 133.05, 132.67, 129.79, 129.22, 59.56, 53.33, 30.24. **MS** m/z $[M-2OH]^{2+}$ calculated, 281.13; found, 281.1292.

Bis[2-(1-methylpiperidyn-1-yl)ethyl]perylene diimide dihydroxide, B2OH.

^{1}H NMR (500 MHz, D_2O) δ 7.87 (d, *J* = 7.7 Hz, 4H), 7.52 (d, *J* = 7.8 Hz, 4H), 3.46 (s, 4H), 3.36 – 3.09 (m, 6H), 3.05 (s, 4H), 1.89 (d, *J* = 36.7 Hz, 16H), 1.68 (s, 4H). **^{13}C NMR** (126 MHz, D_2O) δ 170.93, 133.04, 132.67, 129.79, 129.22, 117.58, 115.25, 59.56, 52.46, 23.30, 20.60, 19.60. **MS** m/z $[M-2OH]^{2+}$ calculated, 321.17; found, 321.1605.

Bis[2-(diisopropyl(methyl))ethyl]perylene diimide dihydroxide, C2OH.

^{1}H NMR (500 MHz, D_2O) δ 7.86 – 7.67 (m, 4H), 7.46 – 7.36 (m, 4H), 3.88 (s, 6H), 3.00 – 2.92 (m, 4H), 2.11 (s, 4H), 1.39 (s, 24H), 0.91 (s, 4H). **^{13}C NMR** (126 MHz, D_2O) δ 160.48, 133.05, 132.69, 129.81, 129.23, 127.51, 127.03, 74.50, 69.09, 59.56, 52.47, 16.89. **MS** m/z $[M\text{-}2OH]^{2+}$ calculated, 337.19; found, 337.1913.

Bis[2-(1,2,6-trimethylpiperidin-1-yl)ethyl]perylene diimide dihydroxide, D2OH.

^{1}H NMR (500 MHz, D_2O) δ 7.78 (d, J = 7.6 Hz, 4H), 7.45 – 7.37 (m, 4H), 4.34 (d, J = 14.8 Hz, 4H), 3.23 (s, 6H), 2.93 (s, 4H), 1.35 (s, 28H). **^{13}C NMR** (126 MHz, D_2O) δ 162.26, 133.02, 132.70, 129.94, 129.33, 117.65, 115.31, 69.04, 65.61, 58.79, 52.47, 34.50, 16.09, 14.52. **MS** m/z $[M\text{-}2OH]^{2+}$ calculated, 349.19; found, 349.1902.

All sample solutions were prepared under an inert N_2 atmosphere in an MBraun glovebox. First, all sources of ambient light were extinguished, and a red LED headlamp was used by the researcher during solution preparation. Pre-weighed samples were dissolved into extra-dry DMF purchased from Sigma Aldrich with a micropipette to produce a 1 mM stock solution which was thoroughly agitated. Aliquots of the stock solution were then diluted to 0.06 mM, 0.05mM, 0.04 mM, 0.03 mM, 0.02 mM, and 0.01 mM. Each sample was placed in a 10 mm threaded screw cap cuvette purchased from Starna Cells, and then capped for fully anaerobic measurement. The caps were replaced after ~4 uses to maintain an airtight seal. Cuvettes were then wrapped with several layers of aluminum foil, taken out of the glovebox, and transported for absorption, transient absorption, and transient photoluminescence. In all cases, care was taken to eliminate sources of light pollution for all measurements. For activation, samples were placed ~30 cm from a 6-LED 405 nm UV lamp with a 60 W power output for 90 mins, or 24 hrs.

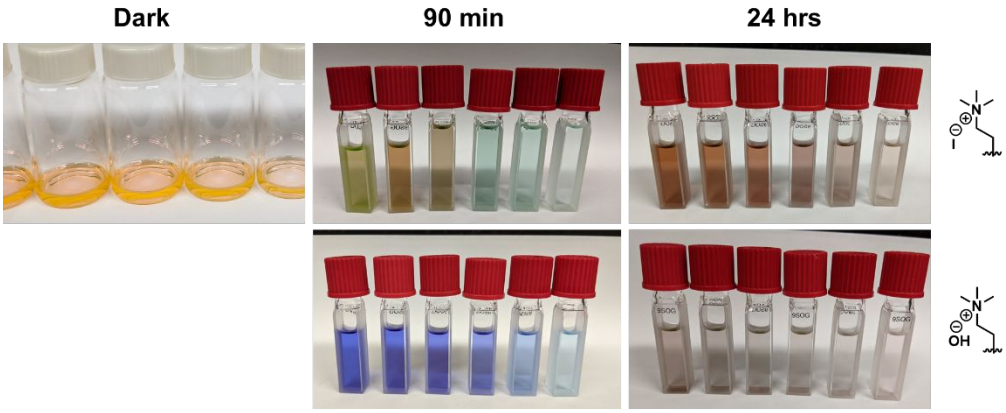

Figure S1. Photochromic behavior of self-n-doped PDIs irradiated at 405 nm. Top left: A2I after 90 mins. Top right: A2I after 24 hrs. Bottom left: A2OH after 90 mins. Bottom right: A2OH after 24 hrs.

Section 2. Absorption studies

All measurements were carried out on a Hitachi U4100 UV-Vis-NIR spectrometer. The 1000-325 nm sampling window was scanned at a rate of 120 nm/min with a sampling interval of 2 nm and a slit width of 1 nm. A gain of 2 dB was used on the PbS detector which dramatically improved the quality of the scans in the NIR spectral region. For easy comparison, all spectra are plotted below (including those that appear in the main body of the manuscript). The percentage of dianion abundance were calculated using a linear regression fit. In the initial integration, a linear fit to the slope of $\mathbf{D}^{\bullet\bullet 2-}$ starting at ~590 nm was taken to zero at ~660 nm, and a linear fit for $\mathbf{R}^{\bullet -}$ starting at ~620 nm to zero at ~570 nm. The two fits were used to then integrate the area of the peaks. The two fits were used to then integrate the area of the peaks. In our new model, the absorbance spectrum (450 nm<λ<1000 nm) for each solution was fit using linear regression to a linear combination of $\mathbf{R}^{\bullet -}$ and $\mathbf{D}^{\bullet\bullet 2-}$ molar attenuation coefficient spectra measured in DMF,

which are known from the work of Gosztola and Wasielewski.[3] Using Beer Lambert's law the molar concentration of $\mathbf{R}^{\bullet-}$, and $\mathbf{D}^{\bullet\bullet 2-}$ were then computed for each solution.

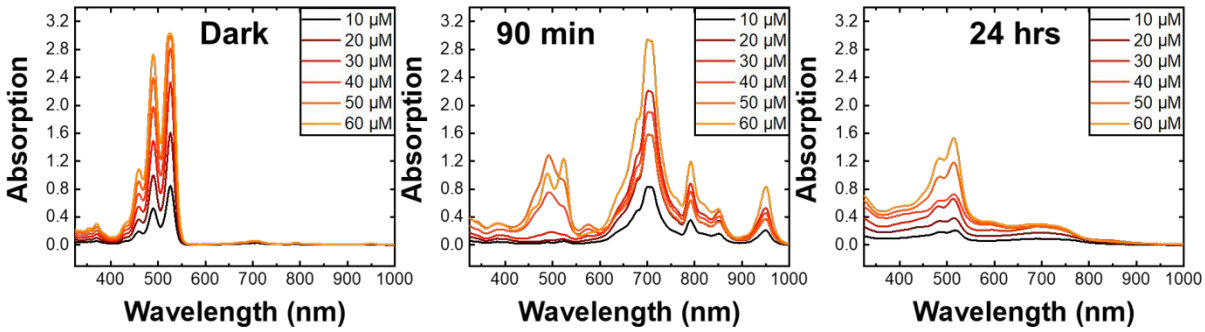

Figure S2. Absorption profiles of A2I in the dark, after 90 mins, and after 24 hrs of photoirradiation.

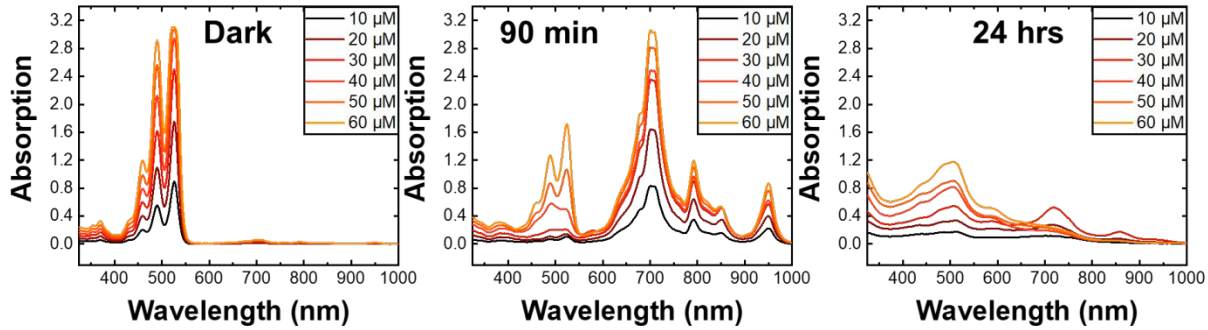

Figure S3. Absorption profiles of B2I in the dark, after 90 mins, and after 24 hrs of photoirradiation.

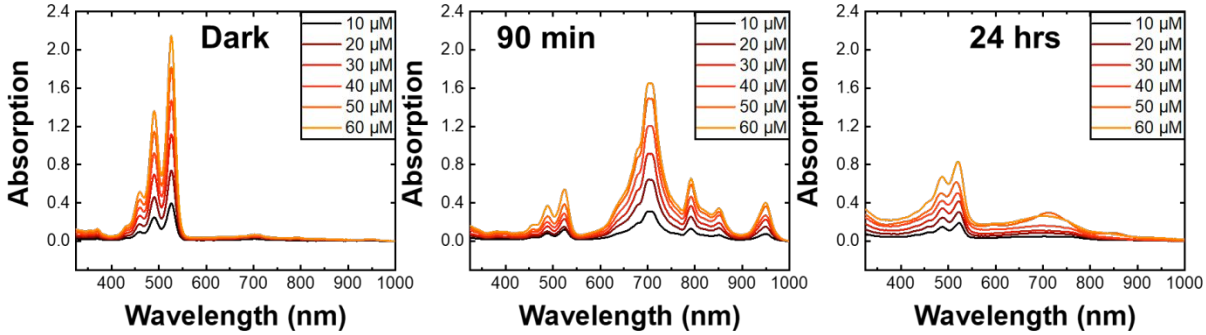

Figure S4. Absorption profiles of C2I in the dark, after 90 mins, and after 24 hrs of photoirradiation.

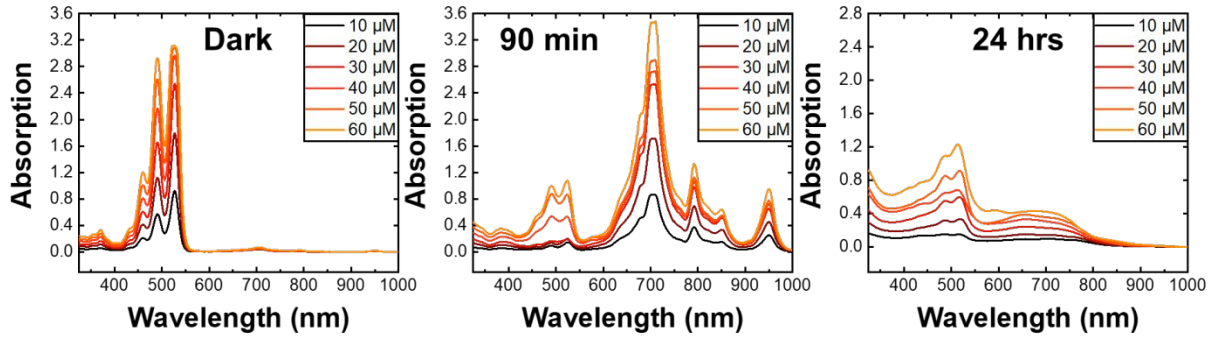

Figure S5. Absorption profiles of D2I in the dark, after 90 mins, and after 24 hrs of photoirradiation.

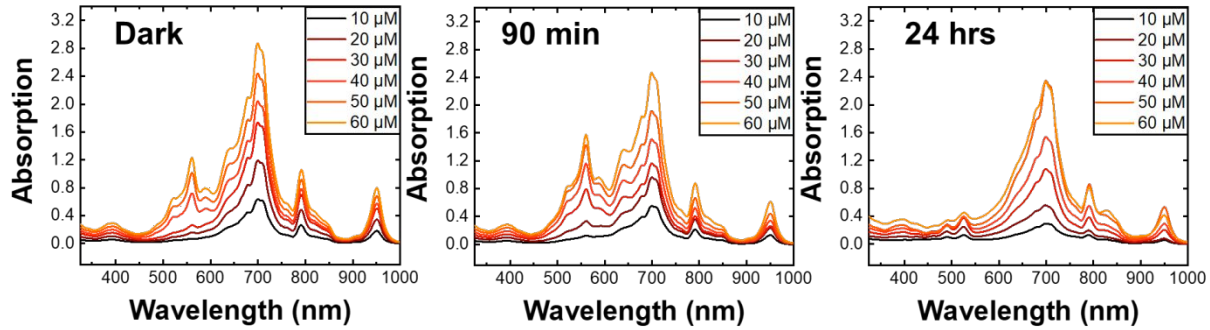

Figure S6. Absorption profiles of A2OH in the dark, after 90 mins, and after 24 hrs of photoirradiation.

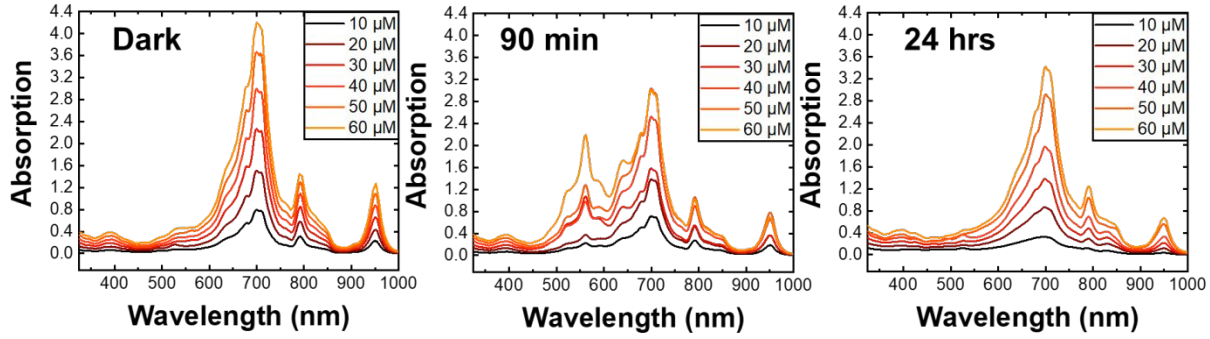

Figure S7. Absorption profiles of B2OH in the dark, after 90 mins, and after 24 hrs of photoirradiation.

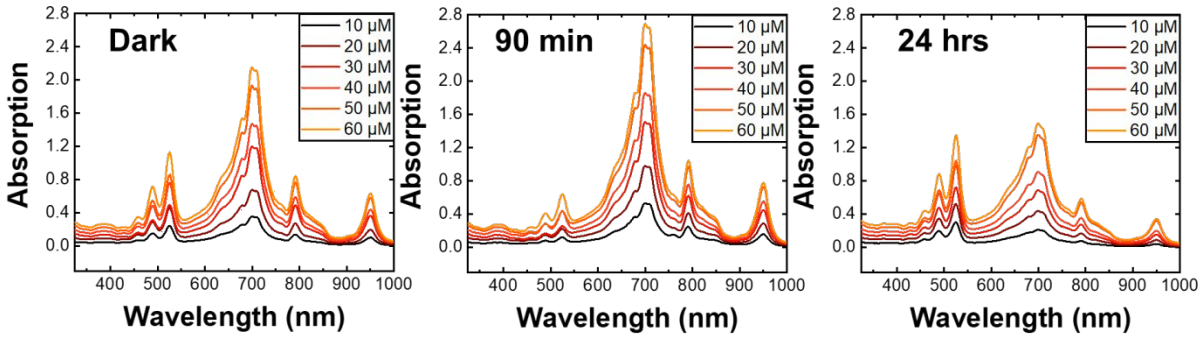

Figure S8. Absorption profiles of C2OH in the dark, after 90 mins, and after 24 hrs of photoirradiation.

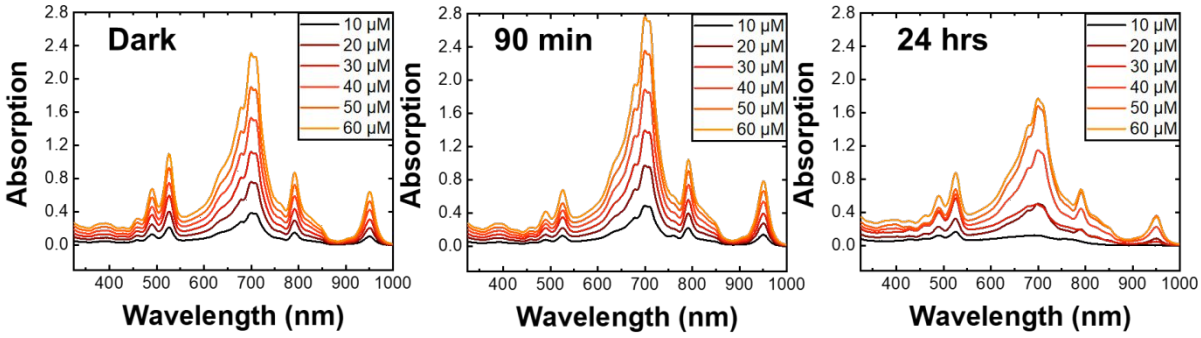

Figure S9. Absorption profiles of D2OH in the dark, after 90 mins, and after 24 hrs of photoirradiation.

Figure S10. linear regression, to a linear combination of $\mathbf{R}^{\bullet-}$ and $\mathbf{D}^{\bullet\bullet 2-}$ molar attenuation coefficient spectra obtained from reported values.[3]

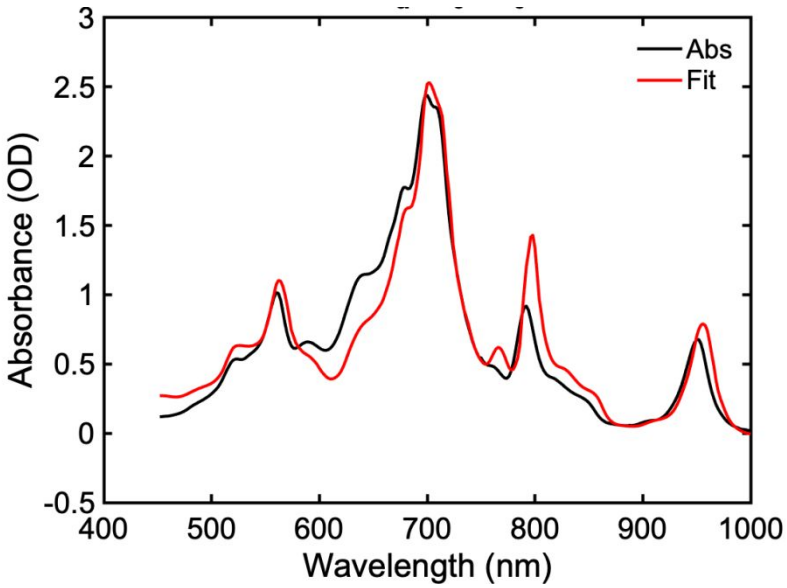

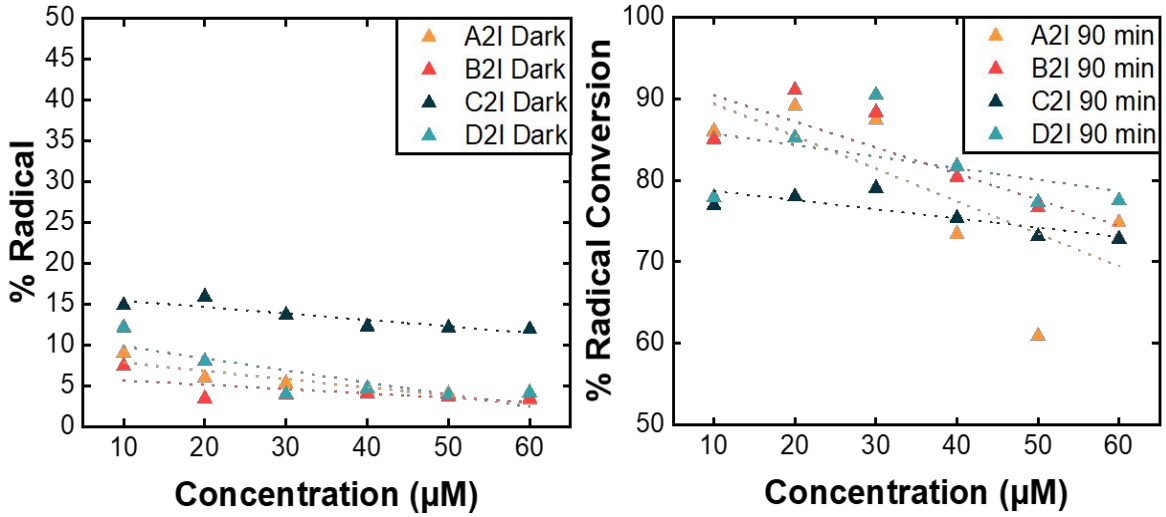

Figure S11. Integrated radical peak area before photoirradiation (left), and percentage radical increase after irradiation (right).

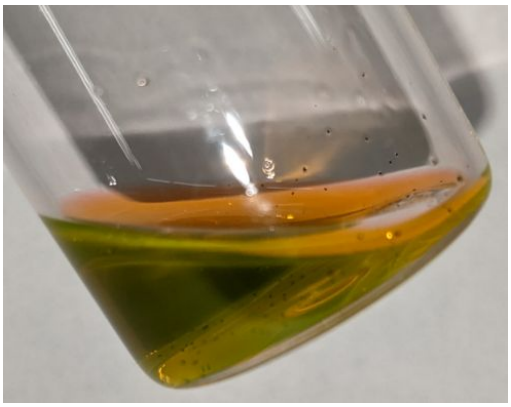

Figure S12. Optical image of 1 mM A2I in DMF after 8 h irradiation.

Section 3. Cyclic voltammetry

Electrochemical measurements were performed using a three-electrode cell with a glassy carbon working electrode (3 mm, CHI Instruments CHI104), silver wire quasi-reference electrode (Ag/Ag^+), and platinum wire counter electrode. The redox characteristics were explored using cyclic voltammetry (CV) measurements with a Biologic VSP potentiostat. All CV experiments were conducted in an argon filled glovebox (MBraun, $\leq 0.5\%$ O_2 and H_2O). Each compound was dissolved to 10 mM in supporting a electrolyte solution (100 mM tetrabutyl ammonium hexafluorophosphate ($TBAPF_6$) in DMF). Solutions were each cycled 3 times, scanning from 0 V vs Ag/Ag^+ at 100 mV s^{-1} to -1.75 V vs Ag/Ag^+ then positively to 2.0 V under dark conditions before illumination and every hour during illumination for 24 hours. Finally, each test was doped with ferrocene as an internal standard reference potential to calibrate the CV measurements vs the ferrocene/ferrocenium reference potential (Fc^0/Fc^+). Non-synthesized compounds were purchased directly from Sigma-Aldrich.

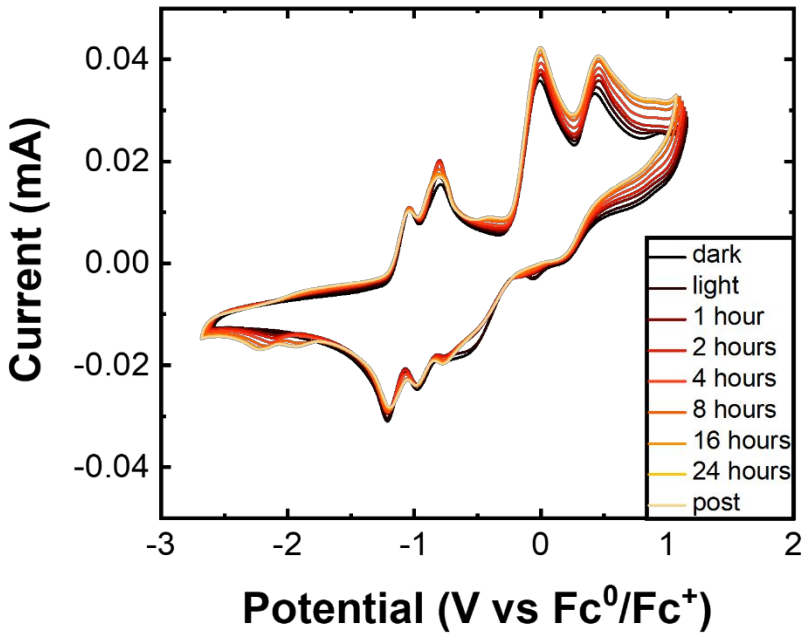

Figure S13. Cyclic voltammograms of B2I in the dark, and at various irradiation timepoints.

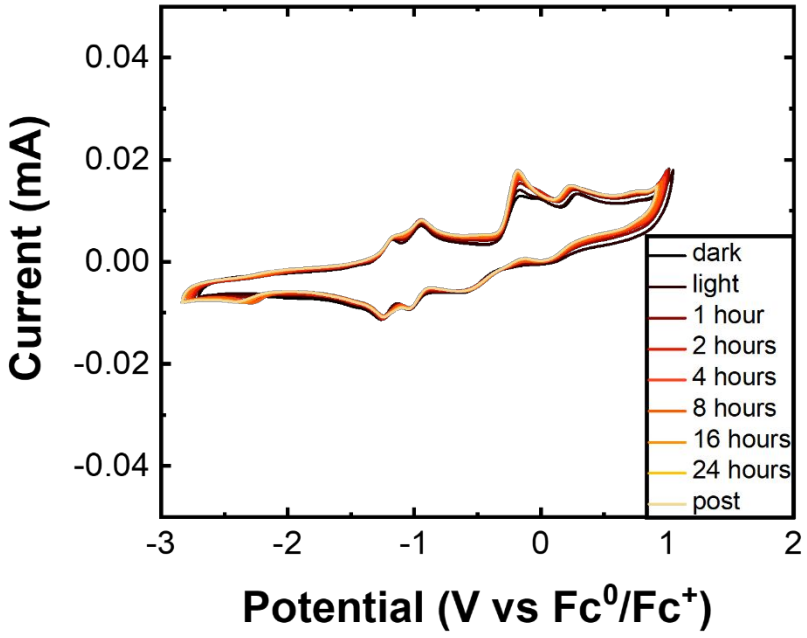

Figure S14. Cyclic voltammograms of C2I in the dark, and at various irradiation timepoints.

Section 4. Femtosecond transient absorption

The pump beam at 400 nm or 520 nm was generated when a 800 nm output of an amplified Ti:sapphire laser (Coherent, Astrella, 5 kHz) pump a collinear optical parametric amplifier (light conversion). The supercontinuum white light was produced in a sapphire plate by focusing a small portion of the laser fundamental. The pump and probe were overlapped in space and time, and a mechanical delay stage was used to control the delay time between pump and probe. The pump power was adjusted around 500μW. The instrument response function was measured to be 100 fs. All the samples were 10 μM and were excited in a 10 mm length cuvette. Note that after 24 hrs of

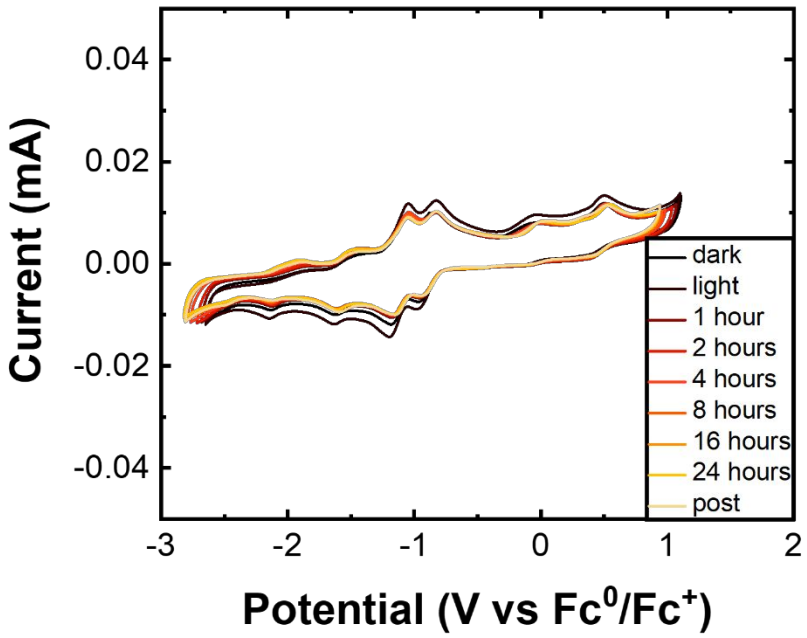

Figure S16. Cyclic voltammograms of B2OH in the dark, and at various irradiation timepoints.

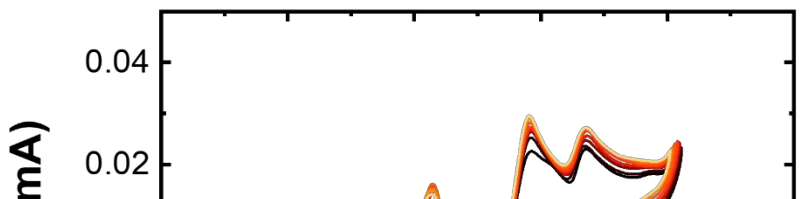

photoirradiation, the transient absorption features remain relatively unchanged though their intensity decreases substantially, which can be plausibly explained by the overall decrease in neutral PDI concentration (refer to brightness changes in section 5) and Mie scattering from the particles suspended in solution. As anticipated, the overall ground state bleach and excited transient absorption intensities decrease with irradiation time due to the conversion PDI→PDI$^{\bullet-}$.

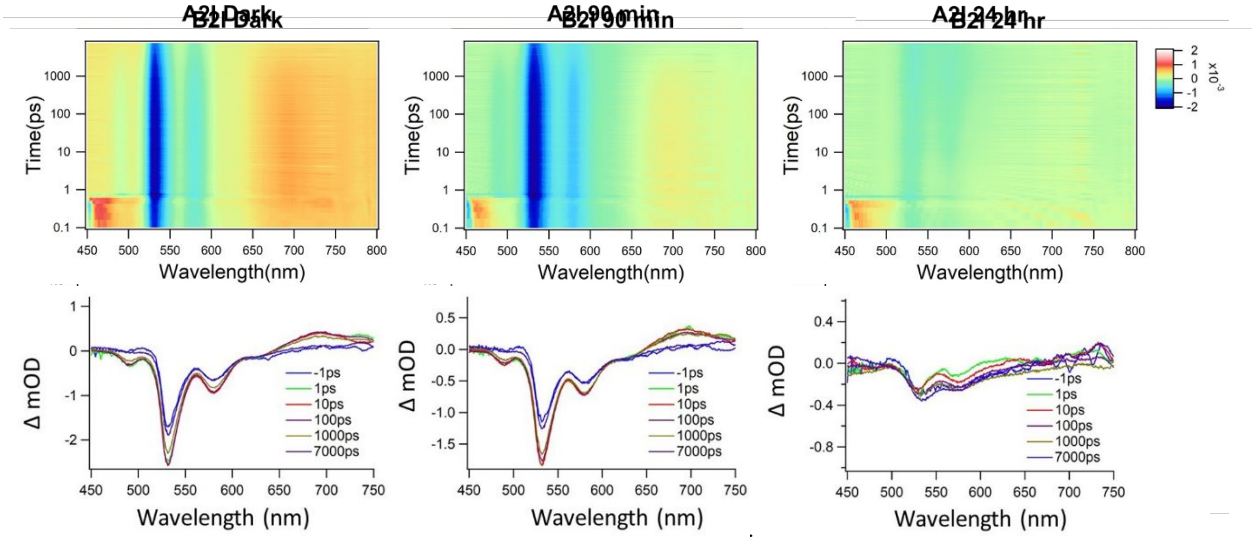

Figure S19. Femtosecond transient absorption maps and time-dependent spectra of A2I.

Figure S20. Femtosecond transient absorption maps and time-dependent spectra of B2I. λ_{ex} = 400 nm; delta mOD is the change in milli-optical density.

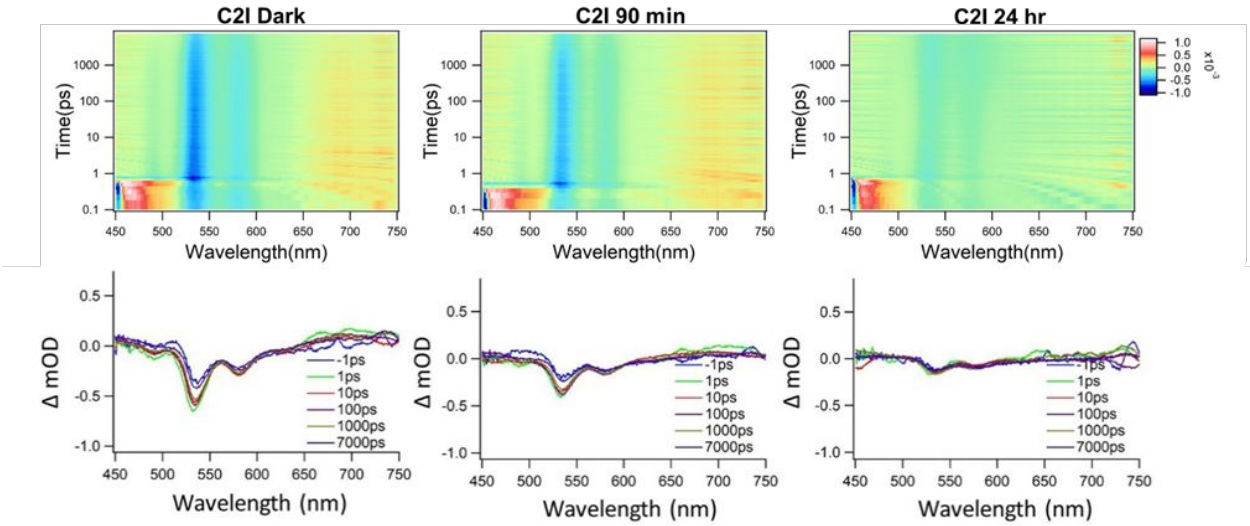

Figure S21. Femtosecond transient absorption maps and time-dependent spectra of C2I. λex = 400 nm; delta mOD is the change in milli-optical density.

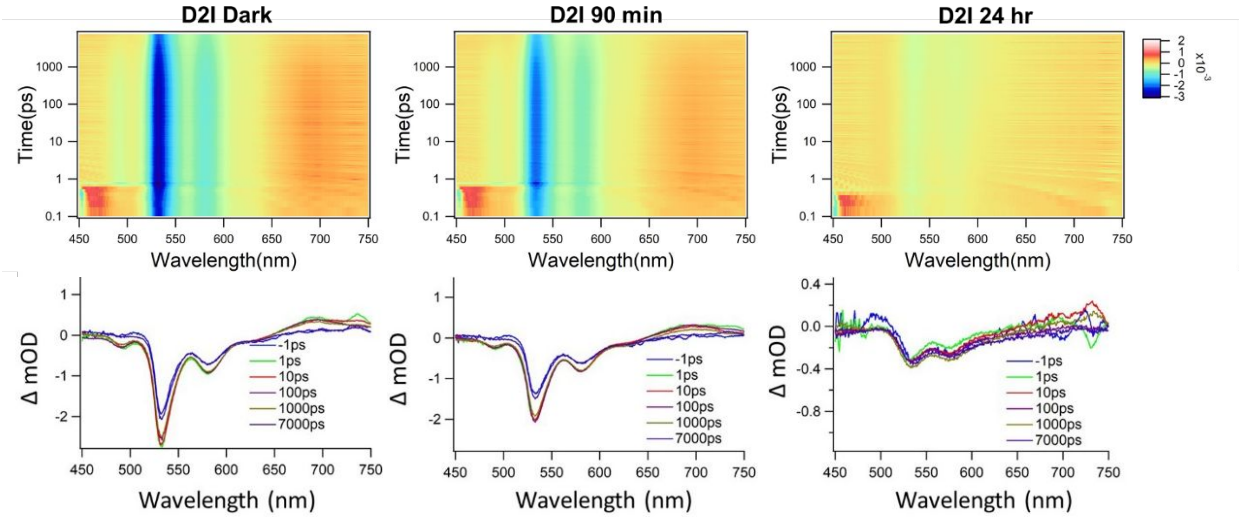

Figure S22. Femtosecond transient absorption maps and time-dependent spectra of D2I. λex = 400 nm; delta mOD is the change in milli-optical density.

Section 5. Time-resolved photoluminescence

Excitation pulses generated from the second harmonic of a tunable Ti:Sapphire laser (Coherent Chameleon Ultra II, 80 MHz repetition rate, <200 fs pulse duration) were centered at 532 nm (FWHM ≤ 3.5 nm) and set to an average power of 83 μW. These vertically polarized pulses were directed to a 562 nm long-pass dichroic and then focused into the sample using an aspheric lens. The fluorescence photons were collected back through the lens and were filtered by the long-pass dichroic and a 20 nm band-pass filter with a central wavelength of 586 nm. Fluorescence was split into two orthogonal polarization channels and collected using identical single-photon Si photodiodes (MPD systems) before being routed to a time-correlated single photon counting module (PHR 800 and Picoharp 300, PicoQuant). Data was collected by integration of counts over 12 s with a resolution of 16 ps.

Table S1. Fluorescence properties of all compounds with iodide counterions.

Total fluorescence			
	BL	A1	τ1 (ns)
A2I Dark	-12,590 ± 148	159,600 ± 100	4.47 ± 0.01
A2I 90 min	-6,975 ± 91	91,920 ± 70	4.37 ± 0.01
A2I 24 hr	-3,843 ± 52	57,100 ± 40	4.23 ± 0.01
B2I Dark	-12,500 ± 140	168,000 ± 100	4.37 ± 0.01
B2I 90 min	-5,663 ± 76	78,810 ± 58	4.30 ± 0.01
B2I 24 hr	-4,880 ± 66	71,310 ± 50	4.25 ± 0.01
C2I Dark	-2,494 ± 43	36,440 ± 35	4.22 ± 0.01
C2I 90 min	-731 ± 20	10,810 ± 15	4.19 ± 0.02
C2I 24 hr	-1,119 ± 25	16,500 ± 20	4.21 ± 0.02
D2I Dark	-11,790 ± 130	165,100 ± 100	4.30 ± 0.01
D2I 90 min	-5,967 ± 75	86,370 ± 60	4.24 ± 0.01
D2I 24 hr	-570 ± 19	7,788 ± 14	4.44 ± 0.03

Anisotropy		
	A1	τ1 (ns)
A2I Dark	0.391 ± 0.004	0.507 ± 0.007
A2I 90 min	0.385 ± 0.005	0.528 ± 0.009
A2I 24 hr	0.383 ± 0.006	0.51 ± 0.01
B2I Dark	0.393 ± 0.004	0.566 ± 0.007
B2I 90 min	0.397 ± 0.005	0.57 ± 0.01
B2I 24 hr	0.380 ± 0.006	0.58 ± 0.01
C2I Dark	0.403 ± 0.008	0.56 ± 0.01
C2I 90 min	0.41 ± 0.01	0.60 ± 0.02
C2I 24 hr	0.39 ± 0.01	0.51 ± 0.02
D2I Dark	0.398 ± 0.003	0.591 ± 0.007
D2I 90 min	0.399 ± 0.005	0.59 ± 0.01
D2I 24 hr	0.40 ± 0.01	0.62 ± 0.04

Section 6. References

Table S2. Fluorescence properties of all compounds with hydroxide counterions.

Total fluorescence			
	BL	A1	τ1 (ns)
A2OH Dark	-548 ± 15	11,130 ± 15	3.78 ± 0.02
A2OH 90 min	-436 ± 15	8,538 ± 14	3.85 ± 0.02
A2OH 24 hr	-1,102 ± 25	15,790 ± 18	4.27 ± 0.02
B2OH Dark	-547 ± 16	10,120 ± 15	3.93 ± 0.02
B2OH 90 min	-275 ± 12	5,280 ± 10	3.90 ± 0.03
B2OH 24 hr	-1,663 ± 30	25,820 ± 25	4.18 ± 0.01
C2OH Dark	-280 ± 12	4,688 ± 10	4.06 ± 0.03
C2OH 90 min	-196 ± 10	3,643 ± 9	3.95 ± 0.03
C2OH 24 hr	-1,108 ± 25	16,970 ± 20	4.20 ± 0.02
D2OH Dark	-2,117 ± 36	40,010 ± 30	3.88 ± 0.01
D2OH 90 min	-1,023 ± 23	21,070 ± 20	3.84 ± 0.01
D2OH 24 hr	-2,676 ± 40	41,700 ± 33	4.15 ± 0.01

Anisotropy		
	A1	τ1 (ns)
A2OH Dark	0.37 ± 0.02	0.43 ± 0.03
A2OH 90 min	0.37 ± 0.02	0.45 ± 0.03
A2OH 24 hr	0.38 ± 0.01	0.47 ± 0.02
B2OH Dark	0.38 ± 0.01	0.57 ± 0.03
B2OH 90 min	0.37 ± 0.02	0.60 ± 0.04
B2OH 24 hr	0.378 ± 0.009	0.58 ± 0.02
C2OH start	0.43 ± 0.02	0.53 ± 0.04
C2OH 90 min	0.42 ± 0.03	0.53 ± 0.04
C2OH 24 hr	0.40 ± 0.01	0.50 ± 0.02
D2OH Dark	0.395 ± 0.007	0.52 ± 0.01
D2OH 90 min	0.39 ± 0.01	0.51 ± 0.02
D2OH 24 hr	0.393 ± 0.007	0.55 ± 0.01

(1) Powell, D.; Campbell, E. v.; Flannery, L.; Ogle, J.; Soss, S. E.; Whittaker-Brooks, L. Steric Hindrance Dependence on the Spin and Morphology Properties of Highly Oriented Self-Doped Organic Small Molecule Thin Films. *Mater. Adv.* **2021**, *2* (1), 356–365. https://doi.org/10.1039/d0ma00822b.

(2) Russ, B.; Robb, M. J.; Brunetti, F. G.; Miller, P. L.; Perry, E. E.; Patel, S. N.; Ho, V.; Chang, W. B.; Urban, J. J.; Chabinyc, M. L.; Hawker, C. J.; Segalman, R. A. Power Factor Enhancement in Solution-Processed Organic n-Type Thermoelectrics through Molecular Design. *Adv. Mater.***2014**, *26* (21), 3473–3477.

(3) Gosztola, D.; Niemczyk, M. P.; Svec, W.; Lukas, A. S.; Wasielewski, M. R. Excited Doublet States of Electrochemically Generated Aromatic Imide and Diimide Radical Anions. *J. Phys. Chem. A* **2000**, *104* (28), 6545–6551.